nanomaterials

MDPI

Article

Constructing Co_3O_4 Nanowire@$NiCo_2O_4$ Nanosheet Hierarchical Array as Electrode Material for High-Performance Supercapacitor

Bo Xu, Lu Pan *, Yaqi Wang and Menglong Liu

School of Chemistry and Materials Engineering, Huainan Normal University, Huainan 232038, China; boxu6673561@sina.com (B.X.); 88wyq1219@sina.com (Y.W.)
* Correspondence: panlu1970@163.com

Abstract: The Co_3O_4 nanowire@$NiCo_2O_4$ nanosheet hierarchical array was constructed on Ni foam using hydrothermal and annealing approaches in turn, from which a $NiCo_2O_4$ nanosheet could self-assemble on the Co_3O_4 nanowire. The structure and morphology of the Co_3O_4 nanowire@$NiCo_2O_4$ nanosheet hierarchical array were characterized via XRD, EDS, SEM, and FESEM, respectively. The electrochemical performance of the composite array was measured via a cyclic voltammetry curve, galvanostatic current charge–discharge, charge–discharge cycle, and electrochemical impedance and then compared with the Co_3O_4 nanowire. The results show that the Co_3O_4 nanowire@$NiCo_2O_4$ nanosheet hierarchical array could reach a high value of 2034 F g^{-1} at a current density of 2.5 A g^{-1}. After 5000 galvanostatic charge–discharge cycles, the specific capacitance of the Co_3O_4 nanowire@$NiCo_2O_4$ nanosheet hierarchical array could still maintain 94.7% of the original value. Therefore, the Co_3O_4 nanowire@$NiCo_2O_4$ nanosheet hierarchical array would be a desirable electrode material for a high-performance supercapacitor.

Keywords: Co_3O_4 nanowire; $NiCo_2O_4$ nanosheets; composites; hierarchical array; supercapacitor

check for updates

Citation: Xu, B.; Pan, L.; Wang, Y.; Liu, M. Constructing Co_3O_4 Nanowire@$NiCo_2O_4$ Nanosheet Hierarchical Array as Electrode Material for High-Performance Supercapacitor. *Nanomaterials* **2024**, *14*, 1703. https://doi.org/10.3390/nano14211703

Academic Editor: Jung Woo Lee

Received: 23 September 2024
Revised: 21 October 2024
Accepted: 22 October 2024
Published: 24 October 2024

Copyright: © 2024 by the authors. Licensee MDPI, Basel, Switzerland. This article is an open access article distributed under the terms and conditions of the Creative Commons Attribution (CC BY) license (https://creativecommons.org/licenses/by/4.0/).

1. Introduction

Co_3O_4 is widely regarded as a promising electrode material for pseudocapacitors due to its high theoretical specific capacitance, low consumption, and environmental friendliness [1–6]. Co_3O_4 nanomaterials with uniform size and special morphology, such as nanosheets, mesoporous nanotubes, and nanospheres, have been reported [7–13]. However, the specific capacitance, energy density, and cyclic performance of pure-phase Co_3O_4 nanoparticles are limited. The exploration of novel Co_3O_4-based nanocomposite electrode materials for supercapacitors have caused extensive research in recent years [14–19]. Co_3O_4-based nanocomposite electrode materials mainly include Co_3O_4@C, Co_3O_4/graphene, Co_3O_4@metal hydroxide, and Co_3O_4@metal oxide [20–27]. Although these Co_3O_4-based nanocomposite electrode materials showed improvement in the supercapacitor electrochemical performance compared with the Co_3O_4 nanostructures, the specific capacitance of these composite electrode materials is not very large, and the energy density is not high. It is still a great challenge to further design multi-component core–shell or heterogeneous electrode materials with higher electrochemical performance and study the corresponding relationship between structure and performance through simple synthesis. The s as-prepared $NiCo_2O_4$ with the similar spinel structure of Co_3O_4 has better electron conductivity, higher electrochemical activity, higher efficiency, lower consumption, and better environmental protection than the traditional transition metal group oxides [28–33]. Recently, an effective method of improving the electrochemical performance of the supercapacitor was to synthesize two metal oxides with similar structures on conductive templates, such as Co_3O_4@$NiMoO_4$ [34,35], Co_3O_4/$NiCo_2O_4$ [36,37], and Co_3O_4@$CoMn_2O_4$ core-shell array structure [38].

In this work, the Co_3O_4 nanowire@$NiCo_2O_4$ nanosheets hierarchical array were constructed on a Ni foam substrate via the hydrothermal method, followed by the annealing

process. The $NiCo_2O_4$ nanosheets are wrapped on the surface of the Co_3O_4 nanowire, which could provide faster ion and electron transfer and improve the structural integrity. The Co_3O_4 nanowire@$NiCo_2O_4$ nanosheets hierarchical array exhibited high specific capacitance and excellent cycling performance, which could be attributed to the synergic effect of the hierarchical nanostructure. The specific capacitance of the Co_3O_4 nanowire@$NiCo_2O_4$ nanosheet hierarchical array could reach 2034 F g^{-1} at a current density of 2.5 A g^{-1} and maintain 94.7% of the original value after 5000 charge–discharge cycles. The Co_3O_4 nanowire@$NiCo_2O_4$ nanosheet hierarchical array showed great potential application in supercapacitors.

2. Experimental Section

All chemical agents were of analytical grade and were used directly without further purification.

2.1. Synthesis of Co_3O_4 Nanowire

A total of 1.50 mmol of $CoCl_2 \cdot 6H_2O$, 1.00 mmol of NH_4F, and 2.00 mmol of urea were dissolved in 40 mL of distilled water under magnetic stirring. The obtained uniform solution was transferred into a 50 mL polytetrafluoroethylene reactor with 2 cm × 3 cm Ni foam and then hydrothermally treated at 120 °C for 6 h. The Ni foam was pre-treated in 6 M HCl. The obtained samples were washed with deionized water and anhydrous ethanol several times. Finally, the washed sample were dried at 60 °C in vacuum and then calcinated at 300 °C for 2 h with a heating rate of 5 °C min^{-1}.

2.2. Synthesis of the Co_3O_4 Nanowire@$NiCo_2O_4$ Nanosheet Hierarchica Array

A total of 0.10 mmol $NiCl_2 \cdot 6H_2O$, 0.20 mmol $CoCl_2 \cdot 6H_2O$, 0.10 mmol NH_4F, and 0.20 mmol urea were accurately weighed and resolved into the mixed solution of 30 mL methanol and 6 mL H_2O; after stirring for 20 min, the uniform solution was transferred to a 50 mL polytetrafluoroethylene reactor with Ni foam-covered Co_3O_4 nanowire and hydrothermally treated at 120 °C for 6 h. The obtained samples were washed with deionized water and anhydrous ethanol several times. Finally, the precursors were dried in a vacuum at 60 °C for 10 h, and final samples were obtained by calcining the precursors at 300 °C for 2 h with a heating rate of 5 °C min^{-1}.

2.3. Characterization of the Co_3O_4 Nanowire@$NiCo_2O_4$ Nanosheet Hierarchica Array

The phase purity of the samples were characterized using an XRD-6000 type X-ray powder diffraction instrument (Shimadzu Corporation, Kyoto, Japan) with a graphite monochromator and high-intensity Cu Ka radiation (λ = 0.154060 nm). The scan speed is 8° min^{-1}. The scan range is 10° to 80°. The field emission scanning electron microscope (FESEM) images of the samples were observed using a Hitachi S-4800 (Tokyo, Japan) field emission scanning electron microscope (accelerated voltage: 5.0 kV). The transmission electron microscope (TEM) images of the samples were observed using a JEOL 2010 (Tokyo, Japan) transmission electron microscope (accelerated voltage: 200 kV).

2.4. Electrochemical Measurement of Samples

The supercapacitor electrochemical performance was measured using a CHI 660D electrochemical workstation (Shanghai Chenhua Instrument Co., Ltd., Shanghai, China). We cut the calcinated Ni foam covering the sample into small pieces of 1 cm × 1 cm. The 1 cm × 1 cm Ni foam covered the sample assembled with a platinum electrode and a standard saturated calomel electrode to form a three-electrode device with the platinum electrode as the counter electrode and the standard saturated calomel electrode as the reference electrode. The cyclic voltammetry curve, galvanostatic charge–discharge, cycling performance, and electrochemical impedance were measured with 3 M KOH solution as the electrolyte.

2.5. Electrochemical Calculation

The electrochemical performance of the specific capacitance Csp of the Co_3O_4 nanowire @$NiCo_2O_4$ nanosheet hierarchical array supercapacitor was calculated via the following formulae:

$$C_{sp} = \frac{\int IdV}{S \times \Delta V \times m},$$

$$C_{sp} = \frac{I \times \Delta t}{m \times \Delta V},$$

where I is the current density of galvanostatic charge and discharge, Δt is the discharge time, m is the mass of the active materials, ΔV is the potential window, and S is the scan speed.

3. Results and Discussion

Structure and Morphology of the Samples

The phase composition of the samples was tested on the X-ray powder diffraction instrument. The results are exhibited in Figure 1. The diffraction peaks of the Co_3O_4 nanowire include the (111), (220), (311), (222), (400), (422), (511), (400), (650), and (533) crystal phases, which can all be indexed to the characteristic peaks of Co_3O_4, indicating that the sample was cubic-phase Co_3O_4 (JCPDS:78-1969). Pure cubic-phase Co_3O_4 nanowire provided the theoretical basis for the preparation of the Co_3O_4 nanowire@$NiCo_2O_4$ nanosheet hierarchical array structure. Compared with the diffraction pattern of the Co_3O_4 nanowire, the diffraction peaks of the Co_3O_4 nanowire@$NiCo_2O_4$ nanosheet hierarchical array demonstrated basically no change except for a slightly enhanced diffraction peak intensity, which can be indexed to the characteristic peaks of spinel-phase $NiCo_2O_4$ (JCPDS:73-1702), indicating formation of the core–shell structure of the Co_3O_4 nanowire@$NiCo_2O_4$ nanosheet hierarchical array.

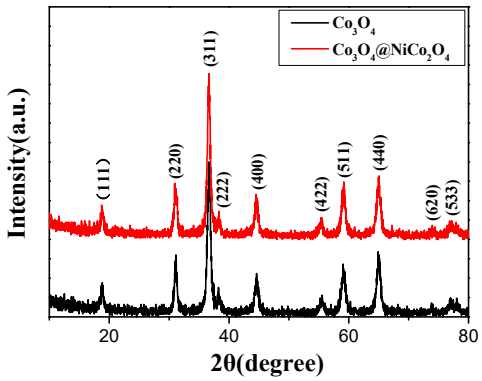

Figure 1. The XRD patterns of the Co_3O_4 nanowire and the Co_3O_4 nanowire@$NiCo_2O_4$ nanosheet hierarchical array.

A field emission scanning electron microscope was used to observe the morphology and size of the samples. Figure 2a,b are the low-magnification and high-magnification SEM images of the Co_3O_4 nanowires. It can be seen that the as-prepared Co_3O_4 nanowire array is rather neat and uniform. Figure 2c,d are low-magnification and high-magnification SEM images of the Co_3O_4 nanowire@$NiCo_2O_4$ nanosheets hierarchical array. A flower-like nanosheet developed and was surrounded tightly by the Co_3O_4 nanowire, and the neat array was formed.

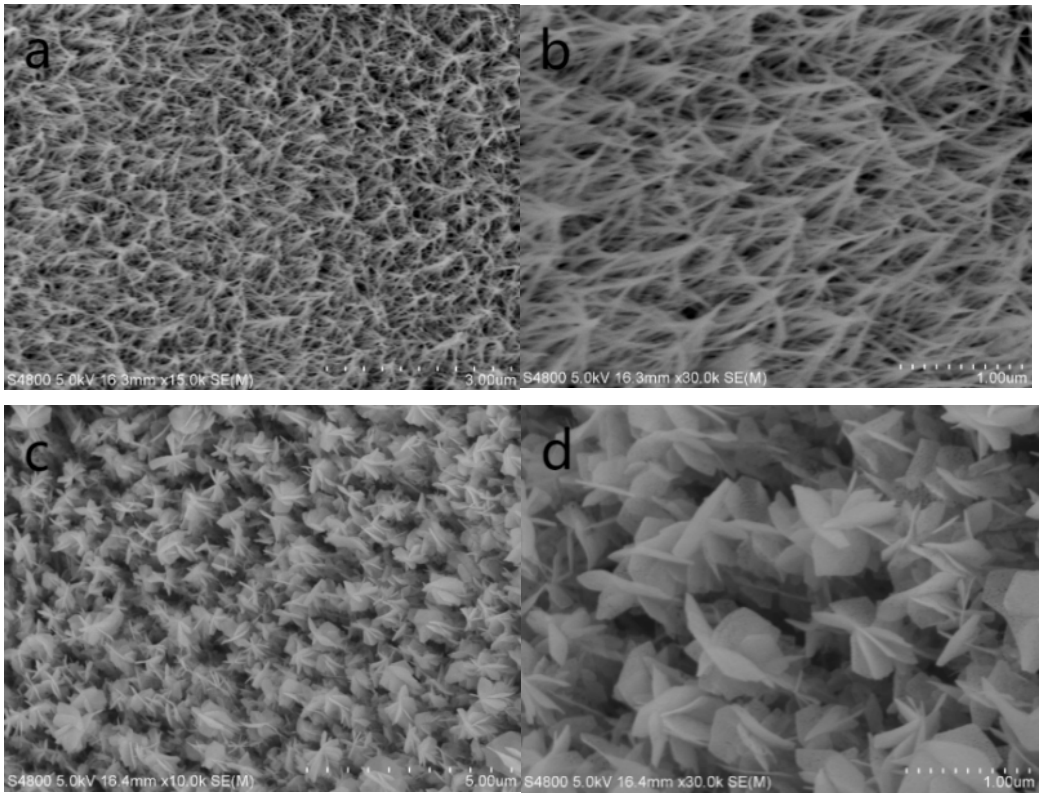

Figure 2. (**a**) Low- and (**b**) high-magnification SEM images of the Co_3O_4 nanowire. (**c**) Low- and (**d**) high-magnification SEM images of the Co_3O_4 nanowire@$NiCo_2O_4$ nanosheet hierarchical array.

The morphology and structure of the samples were further analyzed via a transmission electron microscopy. As can be seen from Figure 3a–c, the constructed Co_3O_4 nanowire array and Co_3O_4 nanowire@$NiCo_2O_4$ nanosheet hierarchical array were all porous in structure, which would increase the number of electrochemical active sites [39,40]. The high-resolution lattice fringes of the samples are shown in Figure 3b–d. The crystal plane spacing of the Co_3O_4 nanowire array was 0.47 nm, corresponding to the (111) crystal plane. The crystal plane spacing of the Co_3O_4 nanowire@$NiCo_2O_4$ nanosheet hierarchical array was 0.245 nm, corresponding to the (111) and (311) crystal planes.

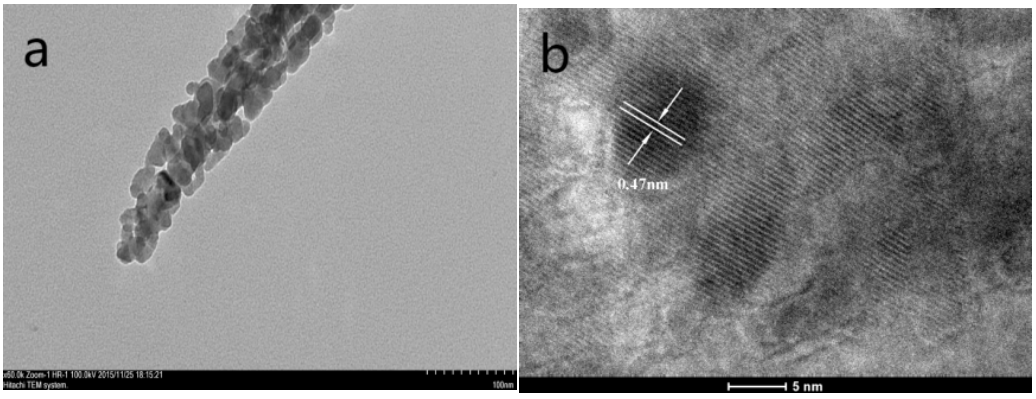

Figure 3. *Cont.*

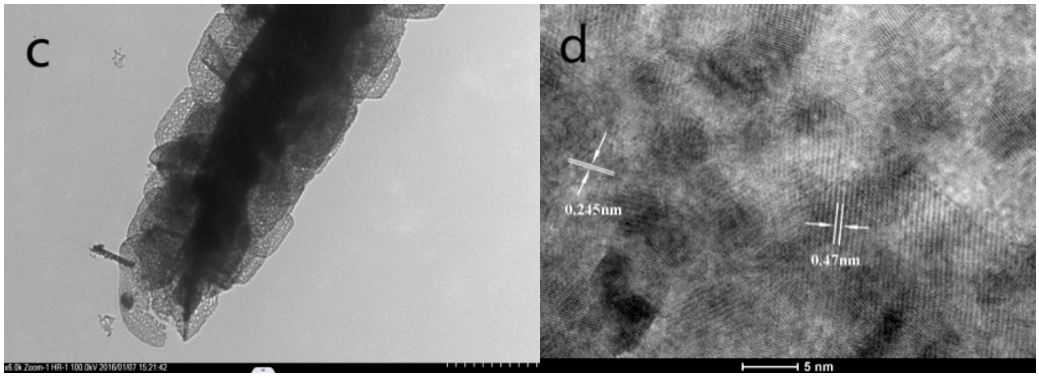

Figure 3. (**a**) TEM and (**b**) HRTEM images of the Co_3O_4 nanowire. (**c**) TEM and (**d**) HRTEM images of theCo_3O_4 nanowire@$NiCo_2O_4$ nanosheet hierarchical array.

The EDS mapping images are shown in Figure 4. Figure 4a shows that there is 18.48 wt% of the Ni element. Figure 4b showed that the Ni element was uniformly distributed. It also confirmed that the $NiCo_2O_4$ nanosheet was successfully constructed on the Co_3O_4 nanowire.

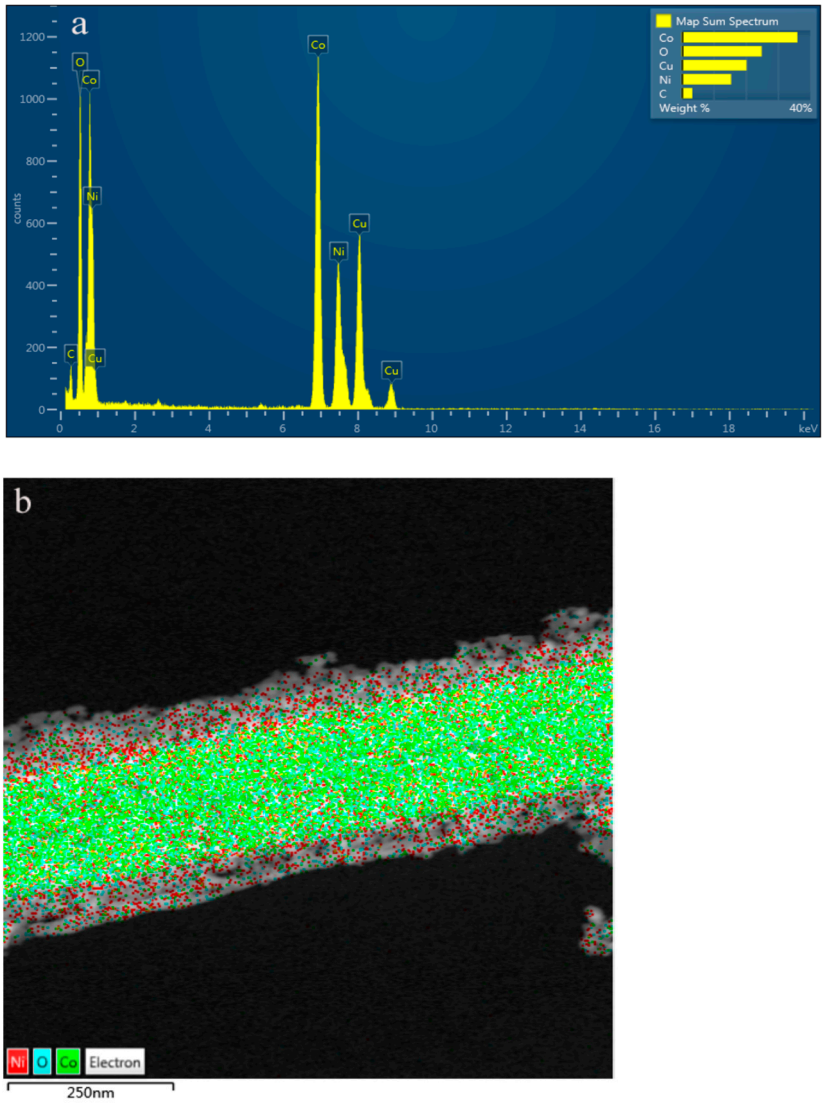

Figure 4. (**a**) Element proportion of the Co_3O_4 nanowire@$NiCo_2O_4$ nanosheet and (**b**) EDS image of the Co_3O_4 nanowire@$NiCo_2O_4$ nanosheet.

The Co_3O_4 nanowire array and the Co_3O_4 nanowire@$NiCo_2O_4$ nanosheet hierarchical array were used as electrode materials to test the supercapacitor electrochemical performance. The results are shown in Figure 5. Cyclic voltammetry curves of the samples were tested under different scan speeds (from 5 to 50 mV s^{-1}) in a voltage range from −0.1 to 0.5 V. The redox peaks in the cyclic voltammetry curves of the Co_3O_4 nanowire electrode material (Figure 5a) are due to the Co^{2+}/Co^{3+} and Co^{3+}/Co^{4+} redox reactions [41,42] (Equations (1) and (2)):

$$Co_3O_4 + OH^- + H_2O = 3CoOOH + e^-, \quad (1)$$

$$CoOOH + OH^- = CoO_2 + H_2O + e^-. \quad (2)$$

For the Co_3O_4 nanowire@$NiCo_2O_4$ nanosheet hierarchical array, the expansion and migration of the redox peak is mainly due to the increase in the Ni^{2+}/Ni^{3+} reaction (Figure 5c) [37] (Equation (3)):

$$NiCo_2O_4 + OH^- + H_2O = NiOOH + 2CoOOH + e^-. \quad (3)$$

According to the above supercapacitor electrochemical calculation (Equation (1)), the specific capacitance values were calculated at different scan speeds. At the scan speeds of 5 mV s^{-1}, 10 mV s^{-1}, 25 mV s^{-1}, and 50 mV s^{-1}, the specific capacitance values of the Co_3O_4 nanowire array were 1267 F g^{-1}, 1108 F g^{-1}, 941 F g^{-1}, and 715 F g^{-1}; and the specific capacitance values of the Co_3O_4 nanowire@$NiCo_2O_4$ nanosheet array were 2642 F g^{-1}, 2473 F g^{-1}, 2234 F g^{-1}, and 1905 F g^{-1}. With the increase in scan speeds, the specific capacitance decreased gradually (Figure 5c). The galvanostatic charge–discharge curves of the samples were tested at different current densities (2.5, 5, 10, and 20 A g^{-1}) in the voltage range of −0.1~0.45 V. The specific capacitance of constant current charge–discharge curves can be calculated according to the above Equation (2). Figure 5b shows the galvanostatic charge–discharge curves of the Co_3O_4 nanowire array. When the current densities were 2.5 A g^{-1}, 5 A g^{-1}, 10 A g^{-1}, and 20 A g^{-1}, the corresponding specific capacitance were 1112 F g^{-1}, 982 F g^{-1}, 834 F g^{-1}, and 680 F g^{-1}. Figure 5d shows the galvanostatic charge–discharge curves of the Co_3O_4 nanowire@$NiCo_2O_4$ nanosheet hierarchical array. When the current densities were 2.5 A g^{-1}, 5 A g^{-1}, 10 A g^{-1}, and 20 A g^{-1}, the specific capacitance values were 2034 F g^{-1}, 1880 F g^{-1}, 1688 F g^{-1}, and 1339 F g^{-1}, respectively (Figure 5d).

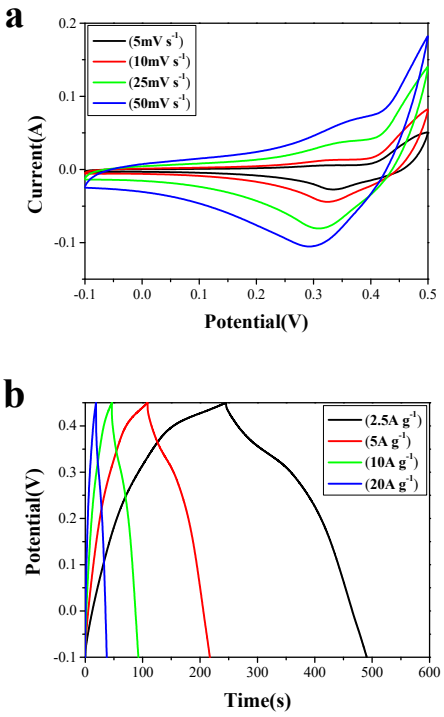

Figure 5. *Cont.*

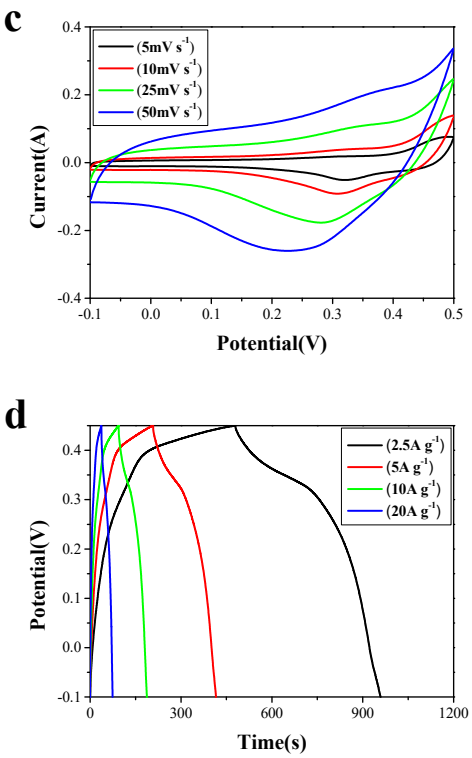

Figure 5. (**a**) Cyclic voltammetry curves of the Co_3O_4 nanowire and (**b**) galvanostatic charge–discharge curves of Co_3O_4 nanowire. (**c**) Cyclic voltammetry curves of the Co_3O_4 nanowire@$NiCo_2O_4$ nanosheet and (**d**) galvanostatic charge–discharge curves of the Co_3O_4 nanowire@$NiCo_2O_4$ nanosheet.

Figure 6a,b shows the comparison of cyclic voltammetry curves of the Co_3O_4 nanowire array and the Co_3O_4 nanowire@$NiCo_2O_4$ nanosheet hierarchical array at a current density of 25 mV s^{-1} and the galvanostatic charge–discharge comparison at a current density of 5 A g^{-1}. The specific capacitance of the Co_3O_4 nanowire@$NiCo_2O_4$ nanosheet hierarchical array was higher than that of the Co_3O_4 nanowire, which may because the two-dimensional nanosheet has a larger BET and has more contact surfaces during the redox reaction of the electrode than the one-dimensional nanowire. The specific capacitance of the Co_3O_4 nanowire@$NiCo_2O_4$ nanosheet hierarchical array was significantly better than that of the Co_3O_4-based nanocomposites reported in the literature, such as Co_3O_4@MnO_2 (1532.4 F g^{-1}, 1 A g^{-1}) [43] and Co_3O_4@$NiCo_2O_4$ (672 F g^{-1}, 0.5 A g^{-1}) [37].

Galvanostatic charge–discharge cycling of the Co_3O_4 nanowire array and the Co_3O_4 nanowire @$NiCo_2O_4$ nanosheet hierarchical array were conducted 5000 times at a current density of 5 A g^{-1} to study the cycling performance. As shown in Figure 6a, the specific capacitance of the Co_3O_4 nanowire array is 91.2%, and that of the Co_3O_4 nanowire @$NiCo_2O_4$ nanosheet hierarchical array is 94.7%. A key factor in the practical application of electrode materials is cycling performance. According to the literature report, the following results obtain: mesoporous Co_3O_4 ultra-thin nanosheets (78.5%, 2000 cycles) [8]; Co_3O_4/MnO_2 (93.4%, 5000 cycles) [43]; and $CoMoO_4$/Co_3O_4 (90.38%, 2000 cycles) [39]. The excellent cycling performance of Co_3O_4 nanowires@$NiCo_2O_4$ nanosheet hierarchical array electrode materials provided a good theoretical basis for practical applications (Table 1).

Table 1. Comparison of cycling performance.

Materials	Capacitance Remaining	Cycles
Co_3O_4 nanowire @$NiCo_2O_4$ nanosheet	94.7%	5000
Co_3O_4 nanowire	91.2%	5000
mesoporous Co_3O_4 ultra-thin nanosheets	78.5%	2000

Table 1. *Cont.*

Materials	Capacitance Remaining	Cycles
Co_3O_4/MnO_2	93.4%	5000
$CoMoO_4/Co_3O_4$	90.38%	2000

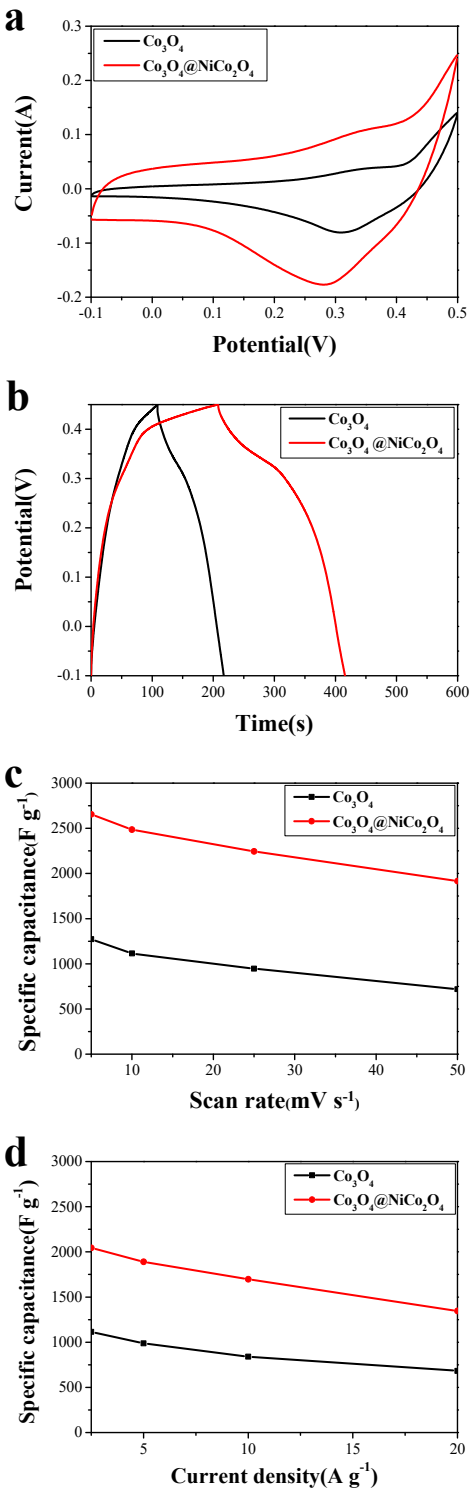

Figure 6. The electrochemical performances comparison of the samples: (**a**) the CVs at 25 mV s^{-1}; (**b**) the charge–discharge curves at 5 A g^{-1}; (**c**) the specific capacitance as a function of scan rate; (**d**) the specific capacitance as a function of current density.

The frequency range of the electrochemical impedance was 100 kHz to 0.05 Hz with the open-circuit voltage of 5 mV (Figure 7). Electrochemical impedance was composed of electrolyte ion resistance, the inherent resistance of the active material, and the contact resistance between the active material and the collector. The diameter of the fitting circle of the quasi-semicircle in the high-frequency region represented the charge transfer resistance of the electrode material in the electrochemical system [44–46]. As shown in Figure 6b, the resistance of the Co_3O_4 nanowire @$NiCo_2O_4$ nanosheet hierarchical array electrode material is significantly lower than that of the Co_3O_4 nanowire array. The lower resistance of charge transfer enables the hierarchical array to have a better electrochemical performance [47,48].

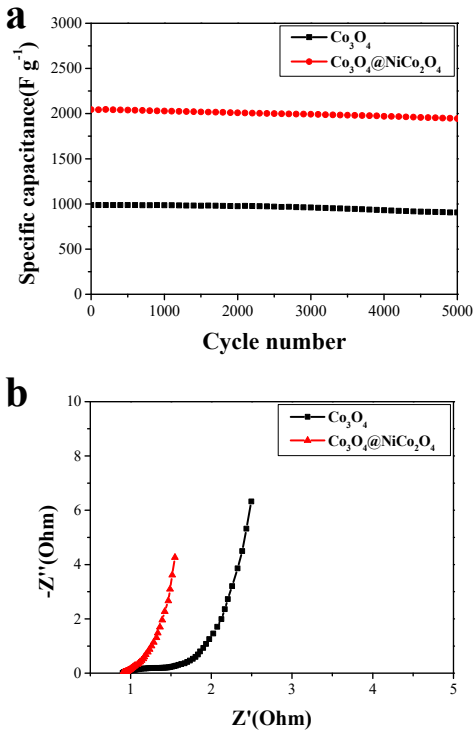

Figure 7. (**a**) The cyclic performance of charge–discharge for 5000 cycles at 5 A g^{-1}. (**b**) Nyquist plots at 1 A g^{-1}.

4. Conclusions

In summary, the Co_3O_4 nanowire@$NiCo_2O_4$ nanosheet hierarchical array was constructed on Ni foam via hydrothermal synthesis followed by calcination treatment. The XRD, SEM, and TEM results demonstrated that the $NiCo_2O_4$ nanosheet wrapped on the surfaces of the Co_3O_4 nanowire provided faster ion and electron transfer and improved structural integrity. The Co_3O_4 nanowire@$NiCo_2O_4$ nanosheet hierarchical array exhibited high specific capacitance and excellent cycling performance. The results showed that the Co_3O_4 nanowire@$NiCo_2O_4$ nanosheet hierarchical array would be a desirable electrode material for a high-performance supercapacitor.

Author Contributions: Methodology, B.X.; Formal analysis, M.L.; Data curation, Y.W.; Writing—review & editing, L.P. All authors have read and agreed to the published version of the manuscript.

Funding: This research received no external funding.

Data Availability Statement: Data are contained within the article.

Conflicts of Interest: The authors declare no conflict of interest.

References

1. Zhu, Y.R.; Peng, P.P.; Wu, J.Z.; Yi, T.F.; Xie, Y.; Luo, S.H. Co_3O_4@$NiCo_2O_4$ microsphere as electrode materials for high-performance supercapacitors. *Solid State Ion.* **2019**, *336*, 110–119. [CrossRef]
2. Yan, A.L.; Wang, W.D.; Wang, B.Q.; Wang, X.C.; Cheng, J.P. Core-shell structured Co_3O_4@$NiCo_2O_4$ nanowires on nickel foam for supercapacitors. *J. Electroanal. Chem.* **2022**, *907*, 116061. [CrossRef]
3. Lu, Y.; Li, L.; Chen, D.; Shen, G.Z. Nanowire-assembled Co_3O_4@$NiCo_2O_4$ architectures for high performance all-solid-state asymmetric supercapacitors. *J. Mater. Chem. A* **2017**, *47*, 6437–6445. [CrossRef]
4. Wang, Y.H.; Che, P.X.; Du, X.Q.; Zhang, X.S. Three-dimensional Co_3O_4@$NiCo_2O_4$ nanoarrays with different morphologies as electrocatalysts for oxygen evolution reaction. *Int. J. Hydrogen Energy* **2020**, *45*, 28598–28606. [CrossRef]
5. Mendoza, R.; Oliva, J.; Rodriguez-Gonzalez, V. Effect of the micro-, meso- and macropores on the electrochemical performance of supercapacitors: A review. *Int. J. Energy Res.* **2022**, *46*, 6989–7020. [CrossRef]
6. Perez-Gonzalez, R.; Cherepanov, S.; Rodriguez-Gonzalez, V.; Mtz-Enriquez, A.I.; Padmasree, K.P.; Zakhidov, A.; Oliva, J. Using $Ca_{2.9}Nd_{0.1}Co_4O_{9+\delta}$perovskites to convert a flexible carbon nanotube based supercapacitor to a battery-like device. *Electrochim. Acta* **2020**, *355*, 136768. [CrossRef]
7. Xu, Y.N.; Ding, Q.; Li, L.; Xie, Z.J.; Jiang, G.X. Facile fabrication of porous Co_3O_4 nanowires for high performance supercapacitors. *New J. Chem.* **2021**, *42*, 20069–20074. [CrossRef]
8. Kang, M.; Zhou, H.; Wen, P.S.; Zhao, N. Highly Hierarchical Porous Ultrathin Co_3O_4 Nanosheets@Ni Foam for High-Performance Supercapacitors. *ACS Appl. Energy Mater.* **2021**, *4*, 1619–1627. [CrossRef]
9. Wei, G.; Yan, L.Q.; Huang, H.F.; Yan, F.X.; Liang, X.Q.; Xu, S.K.; Lan, Q.; Zhou, W.Z.; Guo, J. The hetero-structured nanoarray construction of Co_3O_4 nanowires anchored on nanoflakes as a high-performance electrode for supercapacitors. *Appl. Surf. Sci.* **2021**, *538*, 147932. [CrossRef]
10. Guo, W.; Lian, X.L.; Tian, Y.M.; Yang, T.; Wang, S. Facile fabrication 1D/2D/3D Co_3O_4 nanostructure in hydrothermal synthesis for enhanced supercapacitor performance. *J. Energy Storage* **2021**, *38*, 102586–102592. [CrossRef]
11. Santos, S.; Babu, R.S.; Lessa, T.S.; Samyn, L.M.; Vinodh, R.; Vivekananth, R.; de Barros, A.L.F. Pyrolysis-assisted synthesis of two-dimensional graphitic carbon nitride nanosheets embedded with transition metal oxide (Ni or Fe) for high-performance asymmetric supercapacitors. *J. Ind. Eng. Chem.* **2024**, *133*, 410–418. [CrossRef]
12. Babu, R.S.; Vinodh, R.; Barros, A.L.F.; Samyn, L.M.; Prasanna, K.; Maier, M.A.; Alves, C.H.F.; Kim, H.-J. Asymmetric supercapacitor based on carbon nanofibers as the anode and two-dimensional copper cobalt oxide nanosheets as the cathode. *Chem. Eng. J.* **2019**, *366*, 390–403. [CrossRef]
13. Zhou, J.; Liu, B.B.; Zheng, H.; Ma, W.Q.; Li, Q.; Xu, C.X. One-step construction of strongly coupled $Co_3V_2O_8$/Co_3O_4/MXene heterostructure via in-situ Co-F bonds for high performance all-solid-state asymmetric supercapacitors. *Rare Met.* **2024**, *43*, 682–691. [CrossRef]
14. Yan, S.; Xu, L.; Jiang, J.; Xiao, H.P.; Li, X.H. An extra-long-life supercapacitor based on Co_3O_4/$NiCo_2O_4$/NiO/C&S composite by decomposition of Co/Ni-based coordination complex. *J. Alloys Compd.* **2018**, *764*, 684–690.
15. Paliwal, M.K.; Meher, S.K. Co_3O_4/$NiCo_2O_4$ Perforated Nanosheets for High-Energy-Density All-Solid-State Asymmetric Supercapacitors with Extended Cyclic Stability. *ACS Appl. Nano Mater.* **2020**, *3*, 4241–4252. [CrossRef]
16. Wang, X.H.; Fang, Y.; Shi, B.; Huang, F.F.; Rong, F.F.; Que, R.H.; Shao, M.W. Fabrication of Isomorphous Co_3O_4@Co_3O_4 Hierarchical Core-Shell Nanoneedles for High-Performance Supercapacitors. *Chem. Sel.* **2017**, *2*, 9267–9276.
17. Lian, X.J.; Guo, W.; Wu, Y.L.; Tian, Y.M.; Wang, S. The structure-stabilized Co_3O_4@Co_9S_8 core-shell nanorods synthesized by in-situ sulfuration of Co_3O_4 for high-performance supercapacitors. *J. Alloys Compd.* **2020**, *865*, 158296–158304. [CrossRef]
18. Mendoza, R.; Balderas-Soto, M.; Suarez, R.G.; Zamora, J.; Mtz-Enriquez, A.I.; Zakhidov, A.; Oliva, J. Role of the MnCoGe alloys to enhance the capacitance of flexible supercapacitors made with electrodes of recycled aluminum and carbon nanotubes. *Synth. Met.* **2024**, *306*, 117654. [CrossRef]
19. Mendoza, R.; Al-Sardar, M.; Oliva, A.I.; Robledo-Trujillo, G.; Rodriguez-Gonzalez, V.; Zakhidov, A.; Oliv, J. Improving the electrochemical performance of flexible carbon nanotubes based supercapacitors by depositing Ni@TiO_2:W nanoparticles on their anodes. *J. Phys. Chem. Solids* **2021**, *155*, 110128. [CrossRef]
20. Paliwal, M.K.; Meher, S.K. Porous Co_3O_4 Nanoarrays as a Novel Positive Electrode Material for Co_3O_4 | | Bi_2O_3 Asymmetric Supercapacitors. *ACS Appl. Nano Mater.* **2019**, *2*, 5573–5586. [CrossRef]
21. Chu, X.F.; Wang, C.; Zhou, L.; Yan, X.Z.; Chi, Y.D.; Yang, X.T. Designed formation of Co_3O_4@$NiCo_2O_4$ sheets-in-cage nanostructure as high-performance anode material for lithium-ion batteries. *RSC Adv.* **2018**, *8*, 39879–39883. [CrossRef] [PubMed]
22. Tao, K.; Yang, Y.J.; Yang, C.; Ma, Q.X.; Han, L. Construction of $NiCo_2O_4$ nanosheet-decorated leaf-like Co_3O_4 nanoarrays from metal–organic framework for high-performance hybrid supercapacitors. *Dalton Trans.* **2019**, *37*, 2907–2913. [CrossRef] [PubMed]
23. Wu, X.; Han, Z.C.; Zheng, X.; Yao, S.Y.; Yang, X.; Zhai, T.Y. Core-shell structured Co_3O_4@$NiCo_2O_4$ electrodes grown on flexible carbon fibers with superior electrochemical properties. *Nano Energy* **2016**, *11*, 5298–5307.
24. Luo, W.T.; Wang, X.Q.; Li, J.Y.; Wang, Y.Q.; Zhang, Y.J.; Meng, F.B. Study on morphology regulation and properties of $NiCo_2O_4$@Co_3O_4 nanocomposites: A facile strategy to obtain high-performance electrode materials. *Colloid Surface A* **2023**, *670*, 131560–131568. [CrossRef]
25. Xu, K.B.; Yang, X.J.; Yang, J.M.; Hu, J.Q. Synthesis of hierarchical Co_3O_4@$NiCo_2O_4$ core-shell nanosheets as electrode materials for supercapacitor application. *J. Alloys Compd.* **2017**, *700*, 247–251. [CrossRef]

26. Shi, Z.T.; Sun, G.; Yuan, R.W.; Chen, W.X.; Wang, Z.; Zhang, L.; Zhan, K.; Zhu, M.; Yang, J.H.; Zhao, B. Scalable fabrication of $NiCo_2O_4$/reduced graphene oxide composites by ultrasonic spray as binder-free electrodes for supercapacitors with ultralong lifetime. *J. Mater. Sci. Technol.* **2022**, *99*, 260–269. [CrossRef]
27. Zhang, N.; Su, C.Y.; Chen, J.L. Recent progress of transition metal-based biomass-derived carbon composites for supercapacitor. *Rare Met.* **2023**, *42*, 769–796. [CrossRef]
28. Chen, D.Z.; Pang, D.; Zhang, S.P.; Song, H.O.; Zhu, W.Q.; Zhu, J.W. Synergistic coupling of $NiCo_2O_4$ nanorods onto porous Co_3O_4 nanosheet surface for tri-functional glucose, hydrogen-peroxide sensors and supercapacitor. *Electrochim. Acta* **2019**, *330*, 135326–135332. [CrossRef]
29. Zhang, G.H.; Wang, T.H.; Yu, X.Z.; Zhang, H.N.; Duan, H.G.; Lu, B.G. Nanoforest of hierarchical Co_3O_4@$NiCo_2O_4$ nanowire arrays for high-performance supercapacitors. *Nano Energy* **2013**, *2*, 586–594. [CrossRef]
30. Wang, Y.; Zhang, M.M.; Li, Y.; Ma, T.J.; Liu, H.; Pan, D.H.; Wang, X.Y.; Wang, A. Rational design 3D nitrogen doped graphene supported spatial crosslinked Co_3O_4@$NiCo_2O_4$ on nickel foam for binder-free supercapacitor electrodes. *Electrochim. Acta* **2018**, *29*, 12–20. [CrossRef]
31. Yu, D.B.; Wu, B.; Ge, L.; Wu, L.; Wang, H.T.; Xu, T.W. Decorating nanoporous ZIF-67-derived $NiCo_2O_4$ shells on a Co_3O_4 nanowire array core for battery-type electrodes with enhanced energy storage performance. *J. Mater. Chem. A* **2016**, *28*, 4286–4293. [CrossRef]
32. Zan, T.; Li, S.Q.; Chen, P.; Dong, K.Z.; Wu, Q.S.; Wu, T. Mesoporous Cubic Nanocages Assembled by Coupled Monolayers with 100% Theoretical Capacity and Robust Cycling. *ACS Cent. Sci.* **2024**, *10*, 1283–1294. [CrossRef] [PubMed]
33. Huai, X.Y.; Liu, J.X.; Wu, X. Cobalt-doped $NiMoO_4$ nanosheet for high-performance flexible supercapacitor. *Chin. J. Struct. Chem.* **2023**, *42*, 100158. [CrossRef]
34. Bu, N.; Xiang, J.; Loy, S.; Yang, W.D.; Di, Y.F.; Zhao, R.D.; Wu, F.F.; Ma, D.M.; Li, M.T.; Li, J. Preparation of three-dimensional Co_3O_4@$NiMoO_4$ nanorods as electrode materials for supercapacitors. *Mater. Chem. Phys.* **2022**, *288*, 126419–126427. [CrossRef]
35. Dong, T.; Li, M.; Wang, P.; Yang, P. Synthesis of hierarchical tube-like yolk-shell Co_3O_4@$NiMoO_4$ for enhanced supercapacitor performance. *Int. J. Hydrogen Energy* **2018**, *43*, 14569–14577. [CrossRef]
36. Li, Y.H.; Zhang, Y.F.; Li, Y.J.; Wang, Z.Y.; Fu, Y.H.; Zhang, X.N.; Chen, Y.H.; Zhang, H.Z.; Li, X.D. Unveiling the dynamic capacitive storage mechanism of Co_3O_4 @$NiCo_2O_4$ hybrid nanoelectrodes for supercapacitor applications. *Electrochim. Acta* **2014**, *145*, 177–184. [CrossRef]
37. Gao, X.; Zhang, Y.X.; Huang, M.; Li, F.; Hua, C.; Yu, L.; Zheng, H.L. Facile synthesis of Co_3O_4@$NiCo_2O_4$ core–shell arrays on Ni foam for advanced binder-free supercapacitor electrodes. *Ceram. Int.* **2014**, *40*, 15641–15646. [CrossRef]
38. Liu, T.J.; Kong, H.; Xiong, J.P.; Wei, G.; Su, Z.Q. A MOF-derived hollow Co_3O_4/$NiCo_2O_4$ nanohybrid: A novel anode for aqueous lithium ion batteries with high energy density and a wide electrochemical window. *Nanoscale* **2022**, *45*, 22–32.
39. Chen, X.B.; Liu, X.; Liu, Y.X.; Zhu, Y.M.; Zhuang, G.C.; Zheng, W.; Cai, Z.Y.; Yang, P.Z. Advanced binder-free electrodes based on $CoMn_2O_4$@Co_3O_4 core/shell nanostructures for high-performance supercapacitors. *RSC Adv.* **2018**, *8*, 31594–31602. [CrossRef]
40. Lu, Y.; Deng, B.L.; Wang, J.X.; Tu, Z.K.; Lu, J.M.; Xiao, X.D.; Xu, G. Nanostructured Co_3O_4 for achieving high-performance supercapacitor. *Mater. Lett.* **2020**, *22*, 129101–129109. [CrossRef]
41. Wang, X.; Deng, C.Y.; Hong, X.D.; Dong, W.; Liang, B. Controllable synthesis of $NiCo_2O_4$, $NiCo_2O_4$/graphene composite and their electrochemical application in supercapacitors. *J. Energy Storage* **2022**, *55*, 105837–105847. [CrossRef]
42. Gao, M.; Wang, W.K.; Rong, Q.; Jiang, J.; Zhang, Y.J.; Yu, H.Q. Porous ZnO-Coated Co_3O_4 Nanorod as a High-Energy-Density Supercapacitor Material. *ACS Appl. Mater. Interfaces* **2018**, *10*, 3163–23173. [CrossRef] [PubMed]
43. Liu, G.; Ma, L.; Liu, Q.M. The preparation of Co_3O_4@MnO_2 hierarchical nano-sheets for high-output potential supercapacitors. *Electrochim. Acta* **2020**, *364*, 137265–137273. [CrossRef]
44. Liu, X.X.; Wu, R.; Wang, Y.; Xiao, S.H.; He, Q.; Niu, X.B.; Blackwood, D.J.; Chen, J.S. Self-supported core/shell Co_3O_4@Ni_3S_2 nanowires for high-performance supercapacitors. *Electrochim. Acta* **2019**, *311*, 221–229. [CrossRef]
45. Zhou, J.J.; Li, Q.; Chen, C.; Li, Y.L.; Tao, K.; Han, L. Co_3O_4@CoNi-LDH core/shell nanosheet arrays for high-performance battery-type supercapacitors. *Chem. Eng. J.* **2018**, *350*, 551–558. [CrossRef]
46. Jiang, M.; Abushrenta, N.; Wu, X.C.; Li, Y.P.; Sun, X.M. Investigation for the synthesis of hierarchical Co_3O_4@MnO_2 nanoarrays materials and their application for supercapacitor. *J. Mater. Sci. Mater. Electron. J.* **2016**, *28*, 1281–1287. [CrossRef]
47. Yan, Y.Q.; Ding, S.X.; Zhou, X.Y.; Hu, Q.; Feng, Y.; Zheng, Q.J.; Lin, D.M.; Wei, X.J. Controllable preparation of core-shell Co_3O_4@CoNiS nanowires for ultra-long life asymmetric supercapacitors. *J. Alloys Compd.* **2021**, *867*, 158941–158951. [CrossRef]
48. Meng, S.C.; Wang, Y.T.; He, J.J.; Quan, W.; Gao, M.H.; Jiang, D.L.; Chen, M. Nanowire-assembled Co_3O_4@NiS core-shell hierarchical with enhanced electrochemical performance for asymmetric supercapacitors. *Nanotechnology* **2020**, *31*, 5403–5411. [CrossRef]

Disclaimer/Publisher's Note: The statements, opinions and data contained in all publications are solely those of the individual author(s) and contributor(s) and not of MDPI and/or the editor(s). MDPI and/or the editor(s) disclaim responsibility for any injury to people or property resulting from any ideas, methods, instructions or products referred to in the content.